Research Square

Preprints are preliminary reports that have not undergone peer review.
They should not be considered conclusive, used to inform clinical practice,
or referenced by the media as validated information.

Hybrid Deep Learning for Week-Ahead Evapotranspiration Forecasting

A. A Masrur Ahmed
University of Southern Queensland
Ravinesh C Deo (ravinesh.deo@usq.edu.au)
University of Southern Queensland https://orcid.org/0000-0002-2290-6749
Qi Feng
Northwest Institute of Eco-Environment and Resources
Afshin Ghahramani
University of Southern Queensland
Nawin Raj
University of Southern Queensland
Zhenliang Yin
Northwest Institute of Eco-Environment and Resources
Linshan Yang
Northwest Institute of Eco-Environment and Resources

Research Article

Keywords: Convolutional neural network, gated recurrent unit, hybrid-deep learning, ET forecasting.

Posted Date: April 21st, 2021

DOI: https://doi.org/10.21203/rs.3.rs-424493/v1

License: This work is licensed under a Creative Commons Attribution 4.0 International License.
Read Full License

Hybrid Deep Learning for Week-Ahead Evapotranspiration Forecasting

A. A. Masrur Ahmed*:

School of Sciences, Centre for Sustainable Agricultural Systems & Centre for Applied Climate Sciences, University of Southern Queensland, Springfield, QLD 4300, AUSTRALIA. Email: AbulAbrarMasrur.Ahmed@usq.edu.au; masrur@outlook.com.au

Ravinesh C. Deo*:

School of Sciences, Centre for Sustainable Agricultural Systems & Centre for Applied Climate Sciences, University of Southern Queensland, Springfield, QLD 4300, AUSTRALIA. Email: ravinesh.deo@usq.edu.au

Qi Feng:

Key Laboratory of Ecohydrology of Inland River Basin, Chinese Academy of Sciences, CHINA

Northwest Institute of Eco-Environment and Resources, Chinese Academy of Sciences, Donggang West Rd 320, Lanzhou, 730000, Gansu Province, CHINA. Email: qifeng@lzb.ac.cn

Afshin Ghahramani:

Centre for Sustainable Agricultural Systems, University of Southern Queensland, Springfield, QLD 4300, AUSTRALIA. Email: afshin.ghahramani@usq.edu.au

Nawin Raj:

Centre for Sciences, University of Southern Queensland, Springfield, QLD 4300, AUSTRALIA. Email: nawin.raj@usq.edu.au

Zhenliang Yin:

Key Laboratory of Ecohydrology of Inland River Basin, Chinese Academy of Sciences, CHINA

Northwest Institute of Eco-Environment and Resources, Chinese Academy of Sciences, Donggang West Rd 320, Lanzhou, 730000, Gansu Province, CHINA. Email: yinzhenliang@lzb.ac.cn

Linshan Yang:

Key Laboratory of Ecohydrology of Inland River Basin, Chinese Academy of Sciences, CHINA

Northwest Institute of Eco-Environment and Resources, Chinese Academy of Sciences, Donggang West Rd 320, Lanzhou, 730000, Gansu Province, CHINA. Email: yanglsh08@lzb.ac.cn

Corresponding Authors* A. A. Masrur Ahmed (AbulAbrarMasrur.Ahmed@usq.edu.au) and Ravinesh C. Deo (ravinesh.deo@usq.edu.au)

ABSTRACT

Reference evapotranspiration (ET) is an integral hydrological factor in soil-plant-atmospheric water balance studies and the management of drought events. This paper proposes a new hybrid-deep learning (DL) approach, combining Convolutional Neural Network (CNN) and Gated Recurrent Unit (GRU) along with Ant Colony Optimization (ACO), for a multi-step (week 1 to 4) daily-ET forecast. The method also assimilates a comprehensive dataset with 52 diverse predictors, *i.e.*, satellite-derived Moderate Resolution Imaging Spectroradiometer (MODIS), ground-based datasets from Scientific Information for Landowners (SILO) and synoptic-scale climate indices (CI). To develop a vigorous CNN-GRU model, a feature selection stage entails the Ant Colony Optimization (ACO) method implemented to improve the ET forecast model for the three selected sites in Australian Murray Darling Basin. The results demonstrate excellent forecasting capability of the hybrid CNN-GRU model against the counterpart benchmark models, evidenced by a relatively small mean absolute error and high efficiency. Overall, this study shows that the proposed hybrid CNN-GRU model successfully apprehends the complex and non-linear relationships between predictor variables and the daily ET.

Keywords: Convolutional neural network, gated recurrent unit, hybrid-deep learning, ET forecasting.

Nomenclature

AA	Advection–Aridity
ACO	Ant Colony Optimization
ANN	Artificial Neural Network
AO	Arctic Oscillation
BOM	Australian Bureau of Meteorology
CCF	Cross Correction Function
CNN	Convolutional Neural Network
CNN-GRU	Hybrid Model integrating the ACO and CNN algorithm with GRU
CNN-LSTM	Hybrid Model integrating the ACO and CNN algorithm with LSTM

CI	Climate Indices
DL	Deep Learning
DMI	Dipole Model Index
ECDF	Empirical Cumulative Distribution Function
ELM	Extreme Learning Machine
EMD	Empirical Mode Decomposition
EMI	El-Nino southern oscillation Modoki index
ENSO	El Niño Southern Oscillation
ET	Evapotranspiration
FAO	Food and Agriculture Organization
FE	Forecasting Error
FFNN	Feed Forward Neural Networks
GB	Giga Bite
GCM	Global Climate Model
GRU	Gated Recurrent Unit
GIOVANNI	Geospatial Online Interactive Visualization and Analysis Infrastructure
KNMI	Royal Netherlands Meteorological Institute
LM	Legates-McCabe's Index
LSTM	Long- short term memory
LS-SVM	Least-squares support vector machines
MAE	Mean Absolute Error
MAPE	Mean Absolute Percentage Error
MARS	Multivariate Adaptive Regression Splines
MDB	Murray-Darling Basin
ML	Machine Learning
MLP	Multi-Layer Perceptron
MLR	Multilinear Regression
MJO	Madden-Julian Oscillation

MODIS	Moderate Resolution Imaging Spectroradiometer
MSE	Mean Squared Error
NOAA	National Oceanic and Atmospheric Administration
NSE	Nash–Sutcliffe Efficiency
PACF	Partial Autocorrelation Function
PM	Penman-Monteith
PT–FC	Priestley–Taylor and Flint–Childs
r	Correlation Coefficient
RF	Random Forest
RMSE	Root-Mean-Square-Error
RNN	Recurrent Neural Network
RRMSE	Relative Root-Mean-Square Error
SD	Standard Deviation
SAM	Southern Annular Mode
SILO	Scientific Information for Landowners
SOI	Southern Oscillation Index
SST	Sea Surface Temperature
SVR	Support Vector Regression
SW	Shuttleworth–Wallace

1.0 Introduction

Reference evapotranspiration (ET) plays a significant role in agriculture, ecosystems, and ecological models (Yin et al., 2017). In hydrological cycles, evapotranspiration links the atmospheric water and surface water flows through water vapor transportation to the atmosphere, which eventually returns as precipitation. Moreover, in terms of water quantity, evapotranspiration holds the second-largest mechanism to precipitation in hydrological cycles (Zou et al., 2019). Considering the importance of ET in global energy balance (Zeng et al., 2019), it is essential to understand the hydrological cycle dynamics in order to continuously monitor stochastic in ET to promote sustainable freshwater usage (Zou et al.,

2019).

The most critical parameters that affect evapotranspiration variability are humidity, wind speed, air temperature, and sunlight duration (Pejić et al., 2015). As the temperature increases, the capacity of water holding by soil and transportation of water vapor increases, which eventually increases the evapotranspiration rates. Moreover, because of the complexities in the land-plant-atmosphere system, actual evapotranspiration is rather challenging to measure. Using the Penman-Monteith method (Allen et al., 1998), reference evapotranspiration is determined as a basis for actual evapotranspiration (Yin et al., 2017). Reference evapotranspiration corresponds to the evapotranspiration percentage of reference plants. ET is potentially responsible for more than 90% of global water losses (Morison et al., 2020). Importantly, ET receives significant attention as it has the greatest influence on agricultural water usage. It is mentionable that, due to climate change, ET has fluctuated in different regions of the world (Piticar et al., 2016). Understanding ET's uncertainty of forecasting and its complex associations in changing climates in different regions, a future forecast model for ET under climate change influences continues to gain attention. Therefore, robust ET forecasts are essential in managing water resource issues under a changing climate and drought situations, particularly, to maintain agricultural water use efficiency.

Understanding land surface processes and vegetation affected by weather and climate are mainly grounded on numerical modelling of surface energy fluxes and the hydrological cycle (Bonan, 2008). Researchers have made efforts to develop different modelling approaches used in agricultural systems to estimate evapotranspiration (Abdullah et al., 2015; Chen et al., 2020; Deo and Şahin, 2015; Mehdizadeh, 2018). The Penman-Monteith (PM) and Shuttleworth–Wallace (SW) models are used to predict evapotranspiration for seasonally varied vegetation (Zhu et al., 2013). These physically sound and rigorous models consider ET's relationships with the net radiation heat flux and soil-surface temperature. These models incorporate mass transfer and energy balance and are widely used around the world. The Priestley–Taylor and Flint–Childs (PT–FC) model is radiation based; the advection–aridity (AA) model is based on meteorological variables. The models can be developed with a small set of measurements (Wei et al., 2019). Although prior ET forecasting studies have adopted conventional machine learning methods, the deep learning method for time series analysis is also getting much attention from many researchers (Olah, 2015; Zeng et al., 2019).

The selection of appropriate predictor variables remains practically a vital part of any model's development, compelling computational intricacy, improving the forecasting accuracy and interpretation of the model's characteristics and nature of the predictors used (Prasad et al., 2018). In this research work, predictor variables from three distinct datasets, namely, the MODIS-satellite images, ground-based SILO data and climate indices are used to train the model. Remotely sensed data, i.e., MODIS had been identified as potential predictors for forecasting solar radiation (Ghimire et al., 2019a) and land surface temperature (Deo and Şahin, 2017). Besides this, the SILO dataset, as a Queensland Government database, is continuously used due to its reliability and accuracy (BOM, 2020). However, different studies have demonstrated the potential applying climate indices (Ali et al., 2019; Nguyen-Huy et al., 2018). Hence, integrating a deep learning hybrid model with satellite-derived products, climate indices, and SILO variables can significantly enhance the potential ET forecasts. However, remotely sensed satellite data are yet to be used to forecast ET, especially using a deep learning model. This paper aims to develop a forecast model that considers the dynamic characteristics of ET time series by means of a hybrid-deep learning approach. The proposed model is able to learn the temporal dependencies of the multivariate ET (and its predictor variables) to generate robust forecasting performance. The paper is presented as follows: Section II elucidates the related work. Section III describes the overview of deep-learning model development. Section IV provides experimental setup and explores the robustness of the proposed model through visual and statistical analysis methods. Finally, the concluding remarks and future prospects of the research work are presented is the last section.

2 Related Works

ET forecasting has a rich literature, but these are addressing the problem of ET forecasting using statistical and conventional machine learning models, including artificial neural networks (ANN) (Traore et al., 2010), Random Forest (Wu et al., 2020) and extreme learning machines (ELM) (Abdullah et al., 2015). Patil and Deka (Patil and Deka, 2016) presented a comprehensive ET assessment method which used ELM model in the Thar Desert, India. The ELM method was compared with Hargreaves equations, ANN, and least-squares support vector machines (LS-SVM). The results revealed that ELM was a simple, yet an effective method with substantial improved ET forecasting. Huo et al., (2012)

concluded that temperature and relative humidity were the most important predictors in their modelling. Abdullah et al. (2015) proved that ELM had an outstanding generalisation performance to predict PM-ET using four complete and incomplete meteorological input combinations for their case study in Iraq.

In contrast to the computational methods described above, deep learning (DL) techniques have become the most popular approach towards modelling sequential data (Ghimire et al., 2019c). Intelligent models based on deep learning must use feature extraction to reveal the compounded associations between predictors and a target variable (Ghimire et al., 2019a). Hence predicting potential evapotranspiration using this algorithm is a useful approach for water resources management. However, the deep learning is yet to be explored within the present study region of Australian Murray Darling Basin.

Numerous DL approaches *viz.* Convolutional Neural Network (CNN), long short-term memory (LSTM), Gated Recurrent Unit (GRU) and Recurrent Neural network (RNN) have been implemented in different fields of time series forecasting including rainfall (Hu et al., 2018), air quality (Du et al., 2018), stream flow (Damavandi et al., 2019) and evapotranspiration (Tikhamarine et al., 2019). Liu *et al.* (2016) used a CNN approach to detect three types of climate extreme, namely the river system dynamics, tropical cyclones, and weather fronts independently. The study revealed that different sets of physical predictor variables were able to classify different climatic events. Zhang *et al.* (2017) implemented a deep belief network for the prediction of precipitation using seven environmental parameters from the previous day. They found a better forecast accuracy than various ML and statistical algorithms. However, there were several days in which the forecasts were unreasonably good. In both hydrology and climatology areas, studies using 1D CNN methods are still scarce (Haidar and Verma, 2018) although CNN appears to outperform traditional machine learning models in many studies, to reach state-of-the-art performance. Despite its high capabilities, deep learning models, such as the CNN, have not been significantly explored in hydrological science.

This study adopts the gated recurrent unit (GRU) neural network as a modified version of the LSTM that has also attracted research attention in many recent problems (Zhang et al., 2018). There appears to be only a few studies on GRU-based models, especially within hydrology (Gao et al., 2020). Convolutional Neural Networks (CNN) is no doubt a useful feature extraction method to improve the

overall predictive process (Ghimire et al., 2019b). Therefore, an integration of CNN with GRU can, in foreseeable possibilities, lead to a robust pre-processing of extensive data that provides a viable option to improve the model's forecasting skill. There has also been recent studies that integrated CNN with LSTM for improved performance, such as Ghimire et al. (2019c) showing superior skill of CNN-LSTM model in a problem of solar radiation prediction. The integration of deep learning (*i.e.*, CNN-GRU) for reference evapotranspiration forecasting, however, is yet to be tested explicitly, with no studies previously verifying the utility of this method for Australia's Murray Darling Basin, which is the focus of the present study.

The objectives of this paper are (1) to develop a hybrid deep learning predictive model (CNN-GRU) to forecast reference evapotranspiration (ET) of three selected study sites in MDB region. A feature selection method on various predictor variables obtained from MODIS satellite sensors, climate indices and SILO products, is enhanced with the ant colony optimization (ACO). (2) To forecast ET for week 1, week 2, week 3 and week 4 ahead periods. (3) To explore the contributory influence of climate indices on the accuracy of the newly developed CNN-GRU model. (4) To benchmark the proposed objective model by comparing shallow machine learning machine and classic deep learning methods to address feature dependency over a specific time.

3 Methodology

3.1 Problems and Motivations

ET forecasting has been a prime issue for making decisions on irrigation scheduling (Yin et al., 2017). In general, ET's estimation is a significant component in water-resources management, irrigation planning, hydrological modelling and assessment (Feng et al., 2017). This study aims to develop an ET -forecast model to anticipate ET's change for a specific time. The ET-forecast model can be described as follows: if t is the daily period where one weekly ET would be forecasted at the scale of $t + 7$ for week 1, $t + 14$ for week 2 ahead of ET forecasting. However, ET forecasting depends on related meteorological variables such as air temperature, evaporation, wind speed, precipitation, and humidity. Figure 2 shows the time series plot of selected predictor variables as an example.

Besides, reference evapotranspiration (ET) is the most important climatic element in water balance next to temperature and precipitation thus has implications in soil water balance, e.g., for

analyses and prediction of plant-available water and irrigation. ET is challenging to measure directly, and in most cases, it is estimated from meteorological data (Thomas, 2000). Moreover, the ET forecasting task is challenging due to rapidly changing weather, and many factors influence it. Considering the issue, an ET forecasting approach based on a hybrid deep learning architecture is implemented in this paper. Many researchers have studied the hybrid learning model, which is a practical approach for forecasting hydrological time-series.

This paper applies the CNN-GRU model, which is a potential approach (Ahmed et al., 2021a; Ahmed et al., 2021b). Some recent studies have demonstrated an enhanced performative integration of CNN with LSTM. However, the integration of three distinct data sets used in this paper was examined for their robustness and performance. In this paper, the applied remotely sensed MODIS dataset captures the land surface state while SILO data considers meteorological data from the land surface. Climate mode indices provide input features related to ET and atmospheric-oceanic states' teleconnections to improve the objective model's skill on ET forecasting.

3.2 Deep ET Forecasting Framework

This section describes the developed hybrid deep-learning method, CNN-GRU, for forecasting the ET. The Ant Colony Optimisation (ACO) algorithm was used to select appropriate features for the model. The proposed method combines one-dimensional CNN and GRU and considers ET data's temporal dependencies. Given the correlations between the ET time series' features and variables up to a specific precedent period, the historical memories of predictor and target variables are crucial, as stated in Figure 4 and Figure 5.

Fig. 4 demonstrates the workflow that we designed for developing deep learning forecasting system workflow. It is evident from Fig.4, that the modelling technique consists of three components: first is the ACO for feature selection, the second is multiple one-dimensional convolutional layers for extracting correlated features learning predictor variables, and the third is the implementation of the Gated Recurrent Unit (GRU) network to capture the long time series dependency. Although there is no method is found to evaluate the contribution of the predictors in advance before developing the model (Tiwari et al., 2016). Although two standard ways of choosing the lagged ET memories and predictor variables for the optimum model (Prasad et al., 2017). They are partial autocorrelation (PACF) and

cross-correlation function (CCF) approaches (reference). A critical background activity in terms of ET lags using PACF is shown in Fig. 4. The figure shows that antecedent monthly delays are significant. Cross-correlation determined the statistical equality between the predictors and the target variable. Fig. 5 shows cross-correlation between predictors and ET for Menindee weather station. A set of relevant input combinations were then calculated from r_{cross} of each predictor with ET. In this figure, the blue line indicates a 95% confidence level of the statistically significant r_{cross}. The correlation of the predictor variables with ET was significant for all stations at lag zero (r_{cross}: 0.25–0.85). From the predictor variables, 15 input variables were selected using the ACO feature selection algorithm.

To exploit the predictor variables' temporal dependence, a multiple one-dimensional CNN is trained to extract input function. The network consists of three layers: the input layer, the fully connected output layer, and a hidden layer(s) between the first two layers. In this work, three layers of CNN, max-pooling layer, and dropout layers were used based on the need. Let us assume a matrix $A = [a1, a2, \ldots, aM]$ of training samples of the inputs, where M is the number of training samples. Moreover, each vector is characterised in d-dimensional space measurement. Now, consider $B = [b1, b2, \ldots bN]$ the output vector linked to A. The 1D-CNN consists of an S number of layers, each layer s ($s = 1, \ldots S$) comprises feature signals and performs both convolution and subsampling processes. While forwarding propagation, the input of each feature signal of layer j is the result of the final output accumulation (after the subsampling) of the previous feature signal ($j-1$) convolved with their proper filters and passed through a non-linear activation function. The extracted features are then concatenated to the GRU model, which learns the dependency features from the time series inputs in forward and backward concurrently.

3.3 Multiple 1-Dimensional CNN (CNN)

This study uses Convolutional Neural Networks (CNN) for input data extraction to create the hybrid CNN-GRU model for multi-step forecasting. CNN's resemble traditional neural networks. However, their connectivity between and inside the neuronal layers varies. In traditional neural networks, each neuron in the previous layer is ultimately linked to all neurones, while single-layer neurones do not contribute to the model's network. CNNs are like Feed Forward Neural Networks (FFNNs) with its three-layer model architecture focused on pooling, convolution, and maximum layer

settings.

The connected layer is employed to estimate objective variables depending on the predictor variable's input features. CNN has proven to be a reliable modelling tool to extract hidden features in inputs and generating filters capturing data features in predictor variables (Oehmcke et al., 2018). To extract the pattern in an objective variable (*i.e.,* ET) and associated predictor variables, each convolutional layer is established as follows (Nunez et al., 2018)

$$h_{ij}^{k} = f\left(\left(Q^{k} * x\right)_{ij} + b_{k}\right) \quad (1)$$

Here, Q^{k} is referred to as the weight of the kernel associated with k^{th} feature map, f is the activation function, and the operator of the convolutional procedure is denoted by star sign ($*$). The rectified linear unit (ReLU) is used as an activation function, and adaptive moment estimation (Adam) is selected as an optimisation algorithm using the grid search approach. The ReLU is described as

$$f(x) = \max(0, x) \quad (2)$$

A one-dimensional convolutional operative was adopted to forecast the 1-Dimensional dataset, which essentially simplifies modelling procedures for real-time forecasting execution.

3.4 GRU for feature dependency learning

Our newly proposed hybrid CNN-GRU model utilises gated recurrent unit (GRU) neural network as the predictive tool after extracting features based on the CNN algorithm. GRU is a distinct type of long short-term memory (LSTM) network presented by Cho et al. (2014). GRU can achieve long-short reliance on declining ignition gradients. Along with similarities, GRU possesses different characteristics from the LSTM. For instance, the GRU owns two gates, namely the update gate and reset gate, whereas the LSTM has three gates (*i.e.,* the input gate, forget gate, and output gate). Fig. 3 shows the structure of the gated recurrent unit network.

In a GRU network, two input features, including the input vector *x(t)* and output vector *h(t-1)*, are present in each layer. The yield of each gate is achieved by logical operation and non-linear transformation of predictors. Moreover, the association between predictors and predictand can be defined as follows:

$$r(t) = \sigma_{g}(W_{r}\mathrm{x(t)} + \mathrm{U}_{r}\mathrm{h(t-1)} + \mathrm{b}_{r}) \quad (3)$$

$$z(t) = \sigma_g\,(W_z \mathrm{x(t)} + \mathrm{U}_z \mathrm{h(t-1)} + \mathrm{b}_z) \quad (4)$$

$$h(t) = \big(1 - z(t)\big)\mathrm{o}(t-1) + z(t)\mathrm{o}\hat{h}(t) \quad (5)$$

$$\hat{h}(t) = \sigma_h\left(W_h x(t) + U_h\big(r(t)\big)\mathrm{oh\ (t-1)}\right) + b_h \quad (6)$$

where $r(t)$ is the reset gate vector, $z(t)$ is defined as the update gate vector, W and U are parameter metrics and vector. σ_h is referred to as a hyperbolic tangent, and σ_g is defined as a sigmoid function. Finally, given the architecture of GRU, the training approach is chosen, which includes backpropagation through time. Based on previous studies, *Adam* optimiser was implemented as it has enhanced expertise.

3.5 ACO algorithm for feature selection

Ant Colony Optimization (ACO) is proposed by Dorigo and Caro (Dorigo and Di Caro, 1999), biologically inspired by colonies of ants' behaviours. In this study, we applied an ACO algorithm for feature selection. The ACO algorithm's theory is as follows: when ants locate a trace of foodstuff, they leave a fragrant substance defined as a pheromone to spot the path. When an ant tries finding food, it follows the path of laid pheromone. Besides, this ant again lay pheromone on the path so that the other ants can find the same route. However, if an ant decides between paths, it prefers the path with high pheromone level, which shows that more ants have gone by the path. It is a matter that the ants follow the shorter path for food; the shorter paths get more fragrant than longer paths. If an ant does not travel a path, then the pheromone evaporates over a certain period. Therefore, pheromone intensity is decreased (Sweetlin et al., 2017), and over time, all ants will follow the shorter way for food. Finally, the "evaporation of pheromone" and "probabilistic selection of paths" provide information to ants to find the shortest food path. The concepts lead to elasticity for resolving optimisation challenges. In brief, an ant can use the information in the other ants to choose a better solution. Fig. 3 shows the steps in the ACO algorithm.

4.0 Experiments

In this section, we explain the three distinct datasets and the framework of the application of models. We used three distinct datasets *viz.* MODIS satellite data, ground-based SILO, and synoptic-scale climate mode indices are totaling 52 variables. The objective model (CNN-GRU) was compared with classical shallow machine learning methods (i.e., SVR) and baseline deep learning methods (i.e.,

LSTM and GRU), and hybrid deep learning methods (CNN-LSTM). Finally, model efficiency and effectiveness are optimised.

4.1 Datasets

The predictor variables were collected from three separate data sources, viz., in this analysis. MODIS-satellite datasets are used to capture the land surface status and flow parameters on regular temporal resolutions; the ground-based SILO repository provides meteorological data in a ready-to-use format for biophysical modelling and climate mode indices datasets related to teleconnections between ET and atmospheric-ocean states to boost the objective. The descriptions of three experimental data sets are as follows (as presented in Table 1).

***MODIS Satellite Dataset*:** The hybrid deep learning model (i.e., CNN-GRU) is based on NASA's repository Geospatial Online Interactive Visualization and Analysis Infrastructure (GIOVANNI) (1/02/2003 to 31/03/2020). The repository GIOVANNI offers a robust online visualisation and analysis platform for geoscience datasets, collecting information from 2000 satellite variables (Chen et al., 2010). Thirty-five predictor variables were obtained from the MERRA-2, GLDAS system. GLDAS represents a high-temporal terrestrial modelling system consisting of a terrestrial surface state. MODIS-aqua provides daily products at high resolution (250 m at nadir), and MERRA-2 (Modern Era Retrospective-analysis for Research and Applications -2) is the most recent atmospheric reanalysis derived by NASA. A list of predictors of the MODIS Satellite can be obtained from https://giovanni.gsfc.nasa.gov.

Scientific Information for Landowners (SILO) Dataset: This research selects nine meteorological variables from Scientific Knowledge for Land-Owners (SILO) to expand the pool of predictor variables, allowing practical application and improved model efficiency. SILO data, managed by Queensland's Department of Environment and Research, are popular for studying the Australian climate system. A list of nine selected variables can be found from https://www.longpaddock.qld.gov.au/silo.

Climate Mode Indices: The role of synoptic-scale, climate-mode indices was important in improving the overall model in previous studies that modelled precipitation, streamflow, and soil moisture (Nguyen-Huy et al., 2018; Prasad et al., 2018). Thirteen climate mode indices are collected from various sources in this study: the National Climate Prediction Centre, Australian Bureau of Meteorology (BOM,

2020), National Oceanic and Atmospheric Administration (NOAA), and KNMI Climate Explorer between 1/03/2003 and 31/03/2020. As the positive SOI is linked to La-Nina and the negative SOI is associated with El-Nino events (Adnan et al., 2016), this study used all these indices due to closely correlated rainfall with lagged SOI values, which showed high predictability of rainfall from August-November. We also consider the Madden-Julian Oscillation (MJO), which is seen to cause considerable variance in tropical weather on monthly and weekly periods (BOM, 2020).

FAO-56 Penman-Monteith Equation: As stated earlier, the Penman-Monteith method is a sound and rigorous model that considers the relationships with the net radiation, all kinds of heat flux surface temperature, the PM method was selected for ET calculation. Mathematically, the Penman-Monteith method is stated as follows:

$$ET = \frac{0.408\Delta(R_n - G) + \gamma \frac{900}{T_{mean}+273} \cup_2 (e_s - e_a)}{\Delta + \gamma(1 + 0.34 \cup_2)} \quad (7)$$

Here ET = reference evapotranspiration (mm); Δ = slope from the curve of vapor-pressure–temperature curve (kPa $^{o}C^{-1}$); R_n = net radiation (MJ m^{-2}); G = soil heat flux (MJ m^2 day^{-1}); γ= psychrometric constant (kPa $\circ C^{-1}$); T_{mean} = average daily air temperature at 2 m ($\circ$C); U_2 = mean daily wind speed at 2 m (ms^{-1}); e_s = saturation vapour pressure (kPa); and e_a = actual vapour pressure (kPa). The calculation procedure of ET is outlined in the FAO-56 manual (Allen et al., 1998). Moreover, the variables used to calculate the ET value were collected from SILO database.

4.2 Experimental Setup and Performance

To achieve a vigorous hybrid deep learning model for ET forecasting, a prime task was to optimise deep learning architecture. This section elucidates the experimental environment of hardware and software used for the model implementation. A multi-steps CNN-GRU model and other comparing deep learning models were developed using open-source deep learning interface Keras with TensorFlow. Moreover, classical shallow machine learning methods were developed using Scikit-learn. The objective model is developed under Intel i7 @ 3.6GHz and 16 GB memory computer. Moreover, the software platform MATLAB is used for the ACO algorithm. However, packages such as *matplotlib* and *season* are used for visualising the forecasted ET.

The ET forecasting framework is further compared with a deep learning approach (i.e., CNN-

LSTM, GRU, LSTM, RNN) and shallow machine learning approaches (i.e., MLP, MARS). They are summarised below. CNN-LSTM is a similar type of objective model. Here, CNN is a one-dimensional convolutional neural network used for feature extraction, and LSTM is demonstrated for the feature dependency of time series data for forecasting. GRU (gated Recurrent Unit), LSTM (Long-short Term Memory), and RNN (Recurrent Neural Network) are three baseline deep learning methods. GRU and LSTM are the most popular variants of RNN. CNN is a widely used one-dimensional method used for time series forecasting.

MLP (Multi-layered perceptron) is a supervised ML algorithm. The MLP consists of an input layer, a hidden layer, and an output layer for processing the time series predictor variables. The MARS (Multivariate adaptive regression splines) model considers the multivariate data with the basic functions of predictor variables to serve the interactive effect of the descriptive terms of predicting and forecasting features (Deo et al., 2017). Decision Trees (DTree) are a non-parametric, supervised system of classification and regression. Decision trees learn from data to approximate a sine curve with if-then-else decision laws. A tree can be a constant approximation. The deeper the tree, the more complicated the rules and the fitter the model. Multiple linear regression (MLR) is a mathematical method that uses many explanatory variables to forecast a variable. Breiman (2001) developed a random forest-based model (RF), including regression and classification algorithm. The basic principle of statistical theory is to collect K-samples regularly and arbitrarily from the initial training sample set N to generate a new set of training samples using the bootstrap resampling process, then creating K decision trees of bootstrap-set random forests.

The prime task of proposed deep learning applications is to set up hyper-parameters and optimisation. Many hyper-parameters need to be addressed to develop an effective deep learning method. Experimentally, the default parameters of Keras are used for network initialisation. The default-training parameters are as follows: epoch numbers are 200, the batch size is 5 and look up size is one. ReLU is used as an activation function for GRU, LSTM, CNN-LSTM, and CNN-GRU. Moreover, *tanh* is used as an activation function for the RNN model. Besides, *Adam* optimiser is used with a learning rate is 0.001. The other optimised GRU model parameters are as follows: the hidden layer unit is 60; the input layer size: 15; output layer size is 1. For all deep learning models' architecture, the number of

hidden layer units ranges between 50 and 80.

As a feature extraction method, three convolution layers were used where each layer has distinct filter and kernel size parameter, say (70, 4), (80, 4), (30, 2). Mean Square Error (MSE) was used as a loss function of the model. The activation function of the output layer is linear. Furthermore, we use a min-max normalisation function to scale the predictor variables between 0 and 1. The missing values are filled using the mean value of the same date as the column. Besides, from the experimental datasets, we pick the first twelve years of data for training 01/02/2003-31/12/2014), select the following three-year data for validation (01/01/2015-31/12/2017) and select the last three-year data for testing (01/01/2017-31/3/2020).

The efficiency of the deep learning hybrid model was evaluated using different performance evaluation criteria such as the Pearson's Correlation Coefficient (*r*), root means square error (*RMSE*), Nash- Sutcliffe efficiency (*NSE*) (Nash and Sutcliffe, 1970), mean absolute error (*MAE*). Due to geographic differences between the study stations, we also employed the relative error-based metrics: *i.e*., relative *RMSE (RRMSE)* and relative *MAE (RMAE)*. Mathematically, these metrics are as follows:

$$r = \left\{ \sum_{\mathrm{i}=1}^{\mathrm{N}} \frac{(ET_{\mathrm{o}} - \overline{ET}_{\mathrm{o}})(ET_f - \overline{ET}_f)}{\sqrt{\sum_{\mathrm{i}=1}^{\mathrm{N}} (ET_{\mathrm{o}} - \overline{ET}_{\mathrm{o}})^2 \ \sum_{\mathrm{i}=1}^{\mathrm{N}} \left(ET_f - \overline{ET}_f\right)^2}} \right\}^2 \tag{8}$$

$$\mathrm{MAE} = \frac{1}{N \sum_{\mathrm{i}=1}^{\mathrm{N}} |ET_{\mathrm{f}} - ET_{\mathrm{o}}|} \tag{9}$$

$$\mathrm{RMSE} = \sqrt{\frac{1}{N \sum_{\mathrm{i}=1}^{\mathrm{N}} (ET_{\mathrm{f}} - ET_{\mathrm{o}})^2}} \tag{10}$$

$$\mathrm{NSE} = 1 - \left[1 - \frac{\sum_{\mathrm{i}=1}^{\mathrm{N}} (ET_f)^2}{\sum_{\mathrm{i}=1}^{\mathrm{N}} \left(ET_o - \overline{ET}_f\right)^2} \right] \tag{11}$$

$$RRMSE = \sqrt{1/N \sum_{\mathrm{i}=1}^{\mathrm{N}} (ET_{\mathrm{f}} - ET_{\mathrm{o}})^2 / (1/N \sum_{i=1}^{N} (ET_o))} x100 \tag{12}$$

$$RMAE \ 1/N \sum_{i=1}^{N} |ET_{\mathrm{f}} - ET_{\mathrm{o}}| / (1/N \sum_{i=1}^{N} (ET_o)) x100 \tag{13}$$

In Eq. (8–12), ET_o and ET_{f} represents the observed and forecasted values for i^{th} test value; $\overline{ET}_o$ and $\overline{ET}_f$ refer to their averages, accordingly, and *N* is defined as the number of observations.

4.3 Single Data Set Forecasting Results

The single data set ET forecasting for week 1–4 ahead period with three distinct data sets is provided in Table 2, which provides *an RMSE* of the comparative deep learning models, shallow machine learning models and our proposed model. According to Table 2, our proposed model is far better than the other comparing models as the baseline shallow and deep learning approach; our proposed model reduces to 1.075 to 1.975mm from week 1–4 ahead ET forecasting using the MODIS-satellite dataset. For the SILO data and Climate Mode Indices, the RMSE values were slightly higher from the MODIS data sets. For example, RMSE value ranges from 1.975 to 2.47mm and 1.945 to 2.845mm for the SILO data and Climate Mode Indices, accordingly. The RMSE value of classic deep learning models (i.e., CNN-LSTM, LSTM, GRU and RNN) is lower than the shallow learning methods. The results show that deep learning models are more useful for ET forecasting than traditional shallow machine learning algorithm for week 1–4 ahead forecasting.

To further test the single-data set forecast performance of CNN-GRU and baseline models in three real-world datasets, we examine CNN-GRU's ET forecasting capacity and the other two selected baseline models over the testing period. Figs. 6(a)(b)(c) compare observed ET and forecasted ET of CNN-GRU, GRU and MLP models at the week-1 ahead forecasting. As shown in the figures, our model's output is better than GRU and MLP models, particularly in wave peak and vale time series. We also note that baseline models' single data forecasting performance is sensitive to different datasets. For example, in the MODIS dataset, the CNN-GRU model has better forecast performance than the SILO and Climate Mode Indices dataset (see Fig. 6(a)). Interestingly, forecasting is like all three types of datasets, which indicates a prospect of integrating the datasets.

In a nutshell, for single data set ET forecasting of time series under different times ahead (week 1–4), the proposed model provides the highest robustness. Moreover, comparing deep learning models is also found useful in the forecasting of ET. However, integrating multi-sourced data sets for ET forecasting is not that simple, but a potential approach to increasing forecasting performance.

4.4 Multi-step Forecasting Results Analysis

The multi-step (week 1–4) ahead ET forecasting performance with three integrated datasets are tabulated in Table3, which provides Person's Correlation Coefficient (r), and Root Mean Square Error

(RMSE) comparative analysis of CNN-LSTM, LSTM, GRU, RNN, shallow ML (i.e., MARS, MLP) and our proposed model CNN-GRU. As shown in Table 3, our proposed model is superior to other approaches in terms of multi-step ahead ET forecasting. Among the study sites, the CNN-GRU model for the Menindee station showed the best performance, considering *r* (0.996) and *RMSE* (0.021), *r* (0.996) and *RMSE* (0.021), *r* (0.996), and *RMSE* (0.021) and *r* (0.996) and *RMSE* (0.021) values for the week 1~week 4 ahead ET forecasting. The performance of this model is followed by the CNN-LSTM, LSTM, and GRU model. Similarly, our proposed model reduces RMSE to 0.212 and 0.323 for Fairfield and Gabo Island sites accordingly (see Tables 3 and 4). However, a site-specific signature in the model accuracy was also evident, with the results for Menindee registering the lowest value of *RMSE* generated by the CNN-GRU model. In terms of *r* also, the CNN-GRU model returned the highest value for Menindee, suggesting that the CNN-GRU model was a potential tool for forecasting ET at 1–4 weeks ahead. Unsurprisingly, following other studies (*e.g.*, (Wen et al., 2019)), this study indicates that as the length of the forecasting period was increased, the model's performance appears to reduce at a significant rate in such a way that the *r*-values reduced by 0.30%, 1.10%, 9.15%, 11% and 15% for the 1–4 weeks of ET forecasting.

Besides model evaluation so far, a further appraisal of our objective model is achieved using empirical cumulative distribution functions (ECDF) of absolute forecast error ($|FE|$), illustrated in Fig. 7. For the week 1 ahead in the case of Menindee station, ~95% of the $|FE|$ values generated by the CNN-GRU model fall within <0.226 m error bracket, followed by a more considerable value for CNN-LSTM (0.415 m), LSTM (0.425 m) and the largest error registered by the RF model (1.586 m). By contrast, the error values were ~1.702 m for the CNN-GRU followed by CNN-LSTM (1.75 m) for week 2 ahead of ET forecasting. However, in week 3 and week 4 of ET forecasting, the $|FE|$ values were ~1.79 m and 1.823m, respectively, for the CNN-GRU model. Besides model evaluation so far, a further appraisal of our objective model is achieved using *NS* and *RRMSE* values. Fig. 8 illustrates the absolute forecast error ($|FE|$) using all the four candidate study sites' implemented models. From Fig. 8, the magnitude of *RRMSE* and *NS* for the objective model (CNN-GRU) for the Menindee station is significant, which clarifies the potential merits of the proposed model. *RRMSE* value less than 4% for week 1 ET forecasting, which is far better than the other associated benchmark models, while the *NS* value ranges

from 0.85 to 0.996. For week 2–4 ET forecast, *RRMSE* values ranged between 20% and 25%, which were best for the proposed model. The analysis revealed that the hybrid CNN-GRU model captures the future ET with higher accuracy.

Fig. 9 shows a scatter plot of the forecasted and observed ET values for different n^{th} (n = 1, 2, 3, 4) week ahead across three stations of Murray Darling Basin with a least square regression line, $y = mx + C$ and the coefficient of determination in each sub-panel. Notably, the objective model (*i.e.*, CNN-GRU) is seen to attain more accurate results with considerably larger r^2 values. The ET forecast with hybrid deep learning model for Menindee station performed significantly. In the case of Menindee, for example, the values for m and r^2 are in reasonably good agreement against the 1:1 line representing the forecasted and observed ET values in such a way that ($m|r^2$) are 1.02|0.990 for the hybrid CNN-GRU model for week 1 ahead of ET forecasting. Moreover, for the week 2–4 ahead of ET forecasting, the CNN-GRU model provided results in significant proximity as Week 2 (ET): 0.84|0.845, Week 3 (ET): 0.85|0.828 and Week 4 (ET): 0.87|0.824. Alternatively, the y-intercept of the regression line was close to trivial, *i.e.,* 0.1022 (Week 1), 0.896 (Week 2), 0.713 (Week 3), and 0.53 (Week 4), revealing the efficacy of the deep learning hybrid method for ET forecasting. For the week 2–4 ahead of ET forecasting, the y-intercept, as expected, deviated from the ideal value of 0, caused by more outliers between simulated and reference values in the testing phase.

The correlation between the observed and forecasted daily evapotranspiration produced by the proposed CNN-GRU model *vs* the corresponding benchmark models (*i.e.,* GRU and LSTM), for the case of Menindee station, is illustrated in Fig. 10. The correlations for the hybrid GRU model are positioned close to the observed ET values for the week 1 forecasting, revealing a high degree of forecasting accuracy. An improvement in the model's forecasting performance was attained by applying the CNN algorithm and implementing the ACO method on a standalone GRU model. The disparity between the forecasted ET and the observed ET values was significantly higher for the MLP and GRU models forecasting, which concur with earlier metrics suggesting a potential inadequacy of ET forecast. The blue circle identifies the improvement from classical MLP to GRU, and finally, the objective CNN-GRU model pointed in the figure that indicated the improvement in forecasting.

Fig. 11 includes the wavelet coherency spectrums between observed and forecasted ET of week

1 using CNN-GRU and GRU model. The findings showed that the underlying existence of variation and periodicity across several time-scale bands of ET trends over the testing period. Wavelet coherence, scaled from 0 to 1, was determined based on Torrence and Webster (Torrence and Webster, 1999). The arrows indicate the relative phase relationship within significant zones of higher correlation. For the CNN-GRU model forecasted ET, the all-year band observed a more robust association from a slight discrepancy at different points. Besides, the standalone GRU shows a low correlation. Between 0.0050-0.0156 normalised frequency displayed no consistent trend during the sample period. The overall assessment indicates precise forecasting of ET using the objective models. Notably, in this study, the ACO algorithm was used to improve predictive models. Therefore, Fig. 12 shows the effect of applying ACO as a pre-processing method of data on the per cent change in RMAE values within the testing ET values incrementally. In terms of week 1 ahead of ET forecasting, the *RMAE* (%) values with CNN-GRU model appeared to decrease by ~10 to 20% for three selected stations. However, for the Menindee station, the amount is the highest (~20%). Similarly, for the week 1 ahead ET forecasting of Fairfield station, the ACO feature-extraction skill reduced the error of ~5%-10%. Moreover, for Deniliquin and Gabo Island study sites, the SSM forecasting for the 1st day ahead evaluated through *RMAE* values decreased by slightly less than 20%. It is worth mentioning that the per cent increase in *RMAE* was ~5% for Menindee for the 30th day ahead SSM forecasting with similar deductions for the other stations.

Our study also suggests that groundwater recharge, deep percolation, and plant uptake, which are essential factors to concentrate evapotranspiration in different layers (Zhu et al., 2013), can be ideal variables to understand ET characteristics better while predicting future changes. The hybrid deep learning approach (i.e., CNN-GRU) incorporated with MODIS satellite-derived data, ground-based SILO data and climate mode indices (representing synoptic climate features) can be a good modelling tool for predicting ET months or other hydrological variables at multi-step lead times, including future use in water resource management and sustainable farming.

5 Conclusion and Future Prospects

Using deep hybrid learning, this study incorporates early warning evapotranspiration forecasting at four weekly steps ahead. The study has a hybrid predictive model (i.e., *CNN-GRU*) with Ant Colony Optimisation implemented in forecasting reference evapotranspiration. The novel approach

combined the convolutional neural network with the gated recurrent unit network. Optimum efficiency. The practicality of the model was tested using three distinct datasets of the Australian Murray Darling Basin. Elucidated by graphical presentations and statistical metrics of forecasted and observed ET, the findings reveal a superior CNN-GRU performance relative to an ensemble of other compering models. The study has the following contributions:

1. The research was a novel approach to using the hybrid CNN-GRU model and the ACO algorithm, especially for the Australian Murray Darling Basin, by presenting constructive research methodologies.
2. The competing model (i.e., CNN-LSTM) and eight benchmarking models (i.e., GRU, LSTM, and MARS) were developed to assess the objective model's predictive performance against statistical score metrics and visual analysis of observed and forecasted ET in the test process. The results revealed that the root means squared error for all competing models was substantially more extensive than the objective model registering 0.126 mm, 0.929mm, 0.962 mm and 0.982 mm for week 1~ week 4 accordingly.
3. The ACO was found as a realistic approach to obtaining the best features from an optimal set of predictor variables, and the hybrid CNN-GRU model significantly improved the forecasting performance of evapotranspiration. Thus, the proposed CNN-GRU model yielded an appropriate degree of accuracy when applied at the weeks ahead ET forecast against classic standalone models.
4. The integration of distinct datasets and application of hybrid CNN-GRU with ACO algorithm at various sites of Murray Darling Basin demonstrated the practical application of the approach accurately.

Furthermore, this study's proposed approach can be further applied in forecasting hydrological variables (i.e., stream flows, ET, and soil moisture) at different time scales. As this analysis has centered on a daily scale forecasting, researchers may also follow a future study to use model-simulated global climate model (GCM) variables to estimate future ET in various agricultural spots under global warming scenarios. Moreover, to improve the model's performance, data decomposition techniques such as empirical mode decomposition (EMD) and improved version of EMD may be applied for extracting the future scenarios of hydrological variables.

Credit authorship contribution statement

A. A. Masrur Ahmed: Writing - original draft, Conceptualization, Methodology, Software, Model development and application. **Ravinesh C. Deo:** Conceptualization, Writing - review & editing, Investigation, Supervision. **Afshin Ghahramani:** Writing - review & editing. **Nawin Raj:** Writing - review & editing, **Qi Feng:** Writing - review & editing. **Zhenliang Yin:** Writing - review & editing, **Linshan Yang:** Writing - review & editing.

Acknowledgments

The research was supported by the Chinese Academy of Science (CAS) and the University of Southern Queensland (USQ) under USQ-CAS Postgraduate Research Scholarship (2019–2021). Data were obtained from MODIS-satellite, SILO and NOAA database, which are duly acknowledged. We also thank the Editor and Reviewers for their insightful comments.

References

Abdullah, S.S., Malek, M.A., Abdullah, N.S., Kisi, O., Yap, K.S., 2015. Extreme learning machines: a new approach for prediction of reference evapotranspiration. Journal of Hydrology, 527: 184-195.

Adnan, M. et al., 2016. Influence of natural forcing phenomena on precipitation of Pakistan. Pakistan Journal of Meteorology Vol, 12(24).

Ahmed, A.A.M. et al., 2021a. Deep Learning Forecasts of Soil Moisture: Convolutional Neural Network and Gated Recurrent Unit Models Coupled with Satellite-Derived MODIS, Observations and Synoptic-Scale Climate Index Data. Remote Sensing, 13(4): 554.

Ahmed, A.M. et al., 2021b. LSTM integrated with Boruta-random forest optimiser for soil moisture estimation under RCP4. 5 and RCP8. 5 global warming scenarios. Stochastic Environmental Research and Risk Assessment: 1-31.

Ali, M., Deo, R.C., Maraseni, T., Downs, N.J., 2019. Improving SPI-derived drought forecasts incorporating synoptic-scale climate indices in multi-phase multivariate empirical mode decomposition model hybridized with simulated annealing and kernel ridge regression algorithms. Journal of Hydrology, 576: 164-184. DOI:10.1016/j.jhydrol.2019.06.032

Allen, R.G., Pereira, L.S., Raes, D., Smith, M., 1998. Crop evapotranspiration-Guidelines for computing crop water requirements-FAO Irrigation and drainage paper 56. Fao, Rome, 300(9): D05109.

BOM, 2020. Bureau of Meteorology.

Bonan, G.B., 2008. Forests and climate change: forcings, feedbacks, and the climate benefits of forests. science, 320(5882): 1444-1449.

Breiman, L., 2001. Random Forests. Machine Learning, 45: 5–32.

Chen, C., Jiang, H., Zhang, Y., Wang, Y., 2010. Investigating spatial and temporal characteristics of harmful Algal Bloom areas in the East China Sea using a fast and flexible method, 2010 18th International Conference on Geoinformatics. IEEE, pp. 1-4.

Chen, Z., Zhu, Z., Jiang, H., Sun, S., 2020. Estimating daily reference evapotranspiration based on limited meteorological data using deep learning and classical machine learning methods. Journal of Hydrology, 591. DOI:10.1016/j.jhydrol.2020.125286

Cho, K. et al., 2014. Learning phrase representations using RNN encoder-decoder for statistical machine translation. arXiv preprint arXiv:1406.1078.

Damavandi, H.G. et al., 2019. Accurate Prediction of Streamflow Using Long Short-Term Memory Network: A Case Study in the Brazos River Basin in Texas. International Journal of Environmental Science and Development, 10(10).

Deo, R.C., Downs, N., Parisi, A.V., Adamowski, J.F., Quilty, J.M., 2017. Very short-term reactive forecasting of the solar ultraviolet index using an extreme learning machine integrated with the solar zenith angle. Environ Res, 155: 141-166.

DOI:10.1016/j.envres.2017.01.035
Deo, R.C., Şahin, M., 2015. Application of the Artificial Neural Network model for prediction of monthly Standardized Precipitation and Evapotranspiration Index using hydrometeorological parameters and climate indices in eastern Australia. Atmospheric Research, 161-162: 65-81. DOI:10.1016/j.atmosres.2015.03.018
Deo, R.C., Şahin, M., 2017. Forecasting long-term global solar radiation with an ANN algorithm coupled with satellite-derived (MODIS) land surface temperature (LST) for regional locations in Queensland. Renewable and Sustainable Energy Reviews, 72: 828-848.
Dorigo, M., Di Caro, G., 1999. Ant colony optimization: a new meta-heuristic, Proceedings of the 1999 congress on evolutionary computation-CEC99 (Cat. No. 99TH8406). IEEE, pp. 1470-1477.
Du, S., Li, T., Yang, Y., Horng, S.-J., 2018. Deep air quality forecasting using hybrid deep learning framework. arXiv preprint arXiv:1812.04783.
Feng, Y., Peng, Y., Cui, N., Gong, D., Zhang, K., 2017. Modeling reference evapotranspiration using extreme learning machine and generalized regression neural network only with temperature data. Computers and Electronics in Agriculture, 136: 71-78. DOI:10.1016/j.compag.2017.01.027
Gao, S. et al., 2020. Short-term runoff prediction with GRU and LSTM networks without requiring time step optimization during sample generation. Journal of Hydrology, 589. DOI:10.1016/j.jhydrol.2020.125188
Ghimire, Deo, Raj, Mi, 2019a. Deep Learning Neural Networks Trained with MODIS Satellite-Derived Predictors for Long-Term Global Solar Radiation Prediction. Energies, 12(12). DOI:10.3390/en12122407
Ghimire, S., Deo, R.C., Raj, N., Mi, J., 2019b. Deep solar radiation forecasting with convolutional neural network and long short-term memory network algorithms. Applied Energy, 253: 113541.
Ghimire, S., Deo, R.C., Raj, N., Mi, J., 2019c. Deep solar radiation forecasting with convolutional neural network and long short-term memory network algorithms. Applied Energy, 253. DOI:10.1016/j.apenergy.2019.113541
Haidar, A., Verma, B., 2018. Monthly Rainfall Forecasting Using One-Dimensional Deep Convolutional Neural Network. IEEE Access, 6: 69053-69063. DOI:10.1109/access.2018.2880044
Hu, C. et al., 2018. Deep Learning with a Long Short-Term Memory Networks Approach for Rainfall-Runoff Simulation. Water, 10(11). DOI:10.3390/w10111543
Huo, Z., Feng, S., Kang, S., Dai, X., 2012. Artificial neural network models for reference evapotranspiration in an arid area of northwest China. Journal of arid environments, 82: 81-90.
Liu, Y. et al., 2016. Application of deep convolutional neural networks for detecting extreme weather in climate datasets. arXiv preprint arXiv:1605.01156.
Mehdizadeh, S., 2018. Estimation of daily reference evapotranspiration (ETo) using artificial intelligence methods: Offering a new approach for lagged ETo data-based modeling. Journal of Hydrology, 559: 794-812. DOI:10.1016/j.jhydrol.2018.02.060
Morison, M., Petrone, R., Wilkinson, S., Green, A., Waddington, J., 2020. Ecosystem scale evapotranspiration and CO2 exchange in burned and unburned peatlands: Implications for the ecohydrological resilience of carbon stocks to wildfire. Ecohydrology, 13(2): e2189.
Nash, J.E., Sutcliffe, J.V., 1970. River flow forecasting through conceptual models part I—A discussion of principles. Journal of hydrology, 10(3): 282-290.
Nguyen-Huy, T., Deo, R.C., Mushtaq, S., An-Vo, D.-A., Khan, S., 2018. Modeling the joint influence of multiple synoptic-scale, climate mode indices on Australian wheat yield using a vine copula-based approach. European Journal of Agronomy, 98: 65-81. DOI:10.1016/j.eja.2018.05.006
Nunez, J.C., Cabido, R., Pantrigo, J.J., Montemayor, A.S., Velez, J.F., 2018. Convolutional neural networks and long short-term memory for skeleton-based human activity and hand gesture recognition. Pattern Recognition, 76: 80-94.
Oehmcke, S., Zielinski, O., Kramer, O., 2018. Input quality aware convolutional LSTM networks for virtual marine sensors. Neurocomputing, 275: 2603-2615. DOI:10.1016/j.neucom.2017.11.027
Olah, C., 2015. Understanding lstm networks, 2015. URL http://colah. github. io/posts/2015-08-Understanding-LSTMs.
Patil, A.P., Deka, P.C., 2016. An extreme learning machine approach for modeling evapotranspiration using extrinsic inputs. Computers and Electronics in Agriculture, 121: 385-392.
Pejić, B., Aksić, M., Mačkić, K., Šekularac, G., 2015. Response of potato to water stress in Southern Serbia. Austin Journal of Irrigation, Austin Publishing Group, 1(1): 1-4.
Piticar, A. et al., 2016. Spatiotemporal distribution of reference evapotranspiration in the Republic of Moldova. Theoretical and Applied Climatology, 124(3-4): 1133-1144.
Prasad, R., Deo, R.C., Li, Y., Maraseni, T., 2017. Input selection and performance optimization of ANN-based streamflow forecasts in the drought-prone Murray Darling Basin region using IIS and MODWT algorithm. Atmospheric Research, 197: 42-63. DOI:10.1016/j.atmosres.2017.06.014
Prasad, R., Deo, R.C., Li, Y., Maraseni, T., 2018. Ensemble committee-based data intelligent approach for generating soil moisture forecasts with multivariate hydro-meteorological predictors. Soil and Tillage Research, 181: 63-81.
Sweetlin, J.D., Nehemiah, H.K., Kannan, A., 2017. Feature selection using ant colony optimization with tandem-run recruitment to diagnose bronchitis from CT scan images. Computer methods and programs in biomedicine, 145: 115-125.

Thomas, A., 2000. Spatial and temporal characteristics of potential evapotranspiration trends over China. International Journal of Climatology: A Journal of the Royal Meteorological Society, 20(4): 381-396.

Tikhamarine, Y., Malik, A., Kumar, A., Souag-Gamane, D., Kisi, O., 2019. Estimation of monthly reference evapotranspiration using novel hybrid machine learning approaches. Hydrological Sciences Journal, 64(15): 1824-1842. DOI:10.1080/02626667.2019.1678750

Tiwari, M., Adamowski, J., Adamowski, K., 2016. Water demand forecasting using extreme learning machines. Journal of Water and Land Development, 28(1): 37-52. DOI:10.1515/jwld-2016-0004

Torrence, C., Webster, P.J., 1999. Interdecadal changes in the ENSO–monsoon system. Journal of climate, 12(8): 2679-2690.

Traore, S., Wang, Y.-M., Kerh, T., 2010. Artificial neural network for modeling reference evapotranspiration complex process in Sudano-Sahelian zone. Agricultural water management, 97(5): 707-714.

Wei, G., Zhang, X., Ye, M., Yue, N., Kan, F., 2019. Bayesian performance evaluation of evapotranspiration models based on eddy covariance systems in an arid region. Hydrology and Earth System Sciences, 23(7): 2877-2895. DOI:10.5194/hess-23-2877-2019

Wen, X. et al., 2019. Two-phase extreme learning machines integrated with the complete ensemble empirical mode decomposition with adaptive noise algorithm for multi-scale runoff prediction problems. J. Hydrol., 570: 167-184.

Wu, M. et al., 2020. Random forest predictive model with uncertainty analysis capability for estimation of evapotranspiration in an arid oasis region. Hydrology Research.

Yin, Z. et al., 2017. Future projection with an extreme-learning machine and support vector regression of reference evapotranspiration in a mountainous inland watershed in north-west China. Water, 9(11): 880.

Zeng, Z. et al., 2019. Changes in Reference Evapotranspiration over Southwest China during 1960–2018: Attributions and Implications for Drought. Atmosphere, 10(11). DOI:10.3390/atmos10110705

Zhang, J., Zhu, Y., Zhang, X., Ye, M., Yang, J., 2018. Developing a Long Short-Term Memory (LSTM) based model for predicting water table depth in agricultural areas. JHyd, 561: 918-929.

Zhang, P., Zhang, L., Leung, H., Wang, J., 2017. A deep-learning based precipitation forecasting approach using multiple environmental factors, 2017 IEEE International Congress on Big Data (BigData Congress). IEEE, pp. 193-200.

Zhu, R., Zheng, H., Wang, E., Zhao, W., 2013. Multi-model ensemble simulation of flood events using Bayesian model averaging, MODSIM2013, 20th Int. Congress on Modelling and Simulation. Modelling and Simulation Society of Australia and New Zealand, pp. 455-461.

Zou, M., Kang, S., Niu, J., Lu, H., 2019. Untangling the effects of future climate change and human activity on evapotranspiration in the Heihe agricultural region, Northwest China. Journal of Hydrology. DOI:10.1016/j.jhydrol.2019.124323

Figures

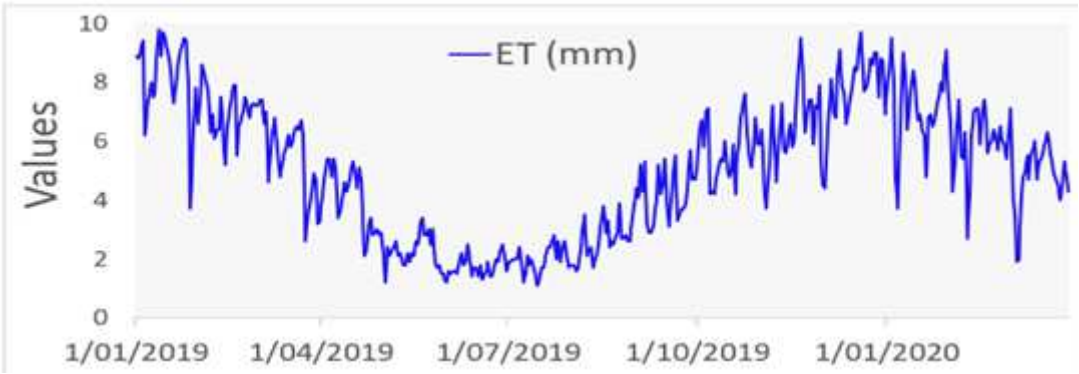


Figure 1

Reference Evapotranspiration (ET) value from January 2019 to March 2020 of Menindee from SILO database.

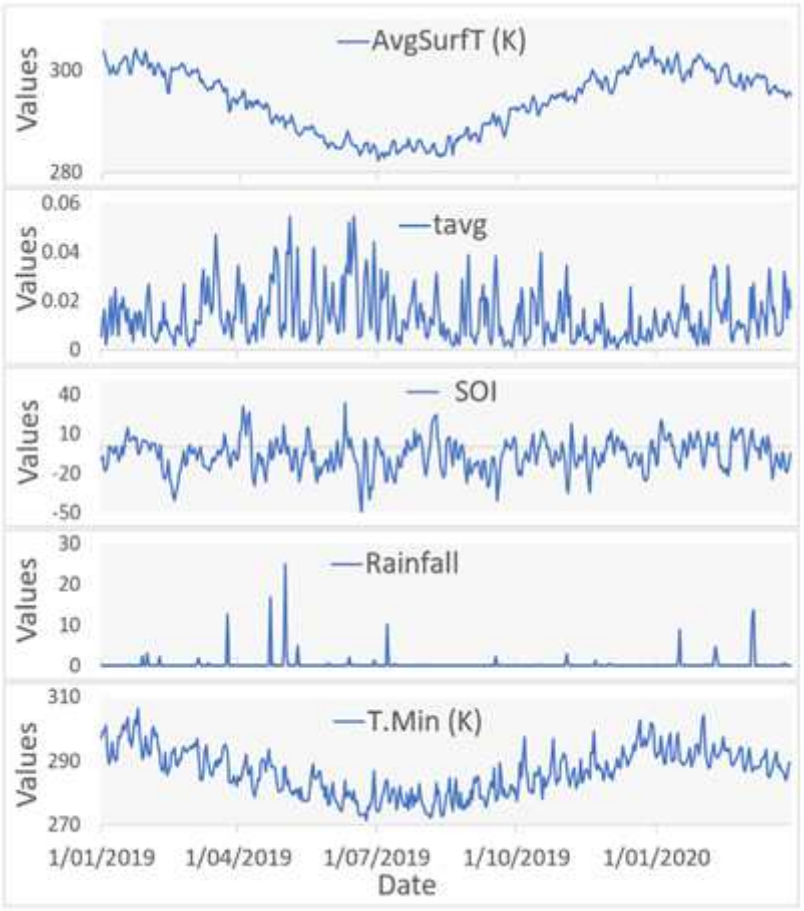


Figure 2

Selected time-series predictors from January 2019 to March 2020 (include avg surface temp, evaporation, SOI, Rainfall, and minimum temperature).

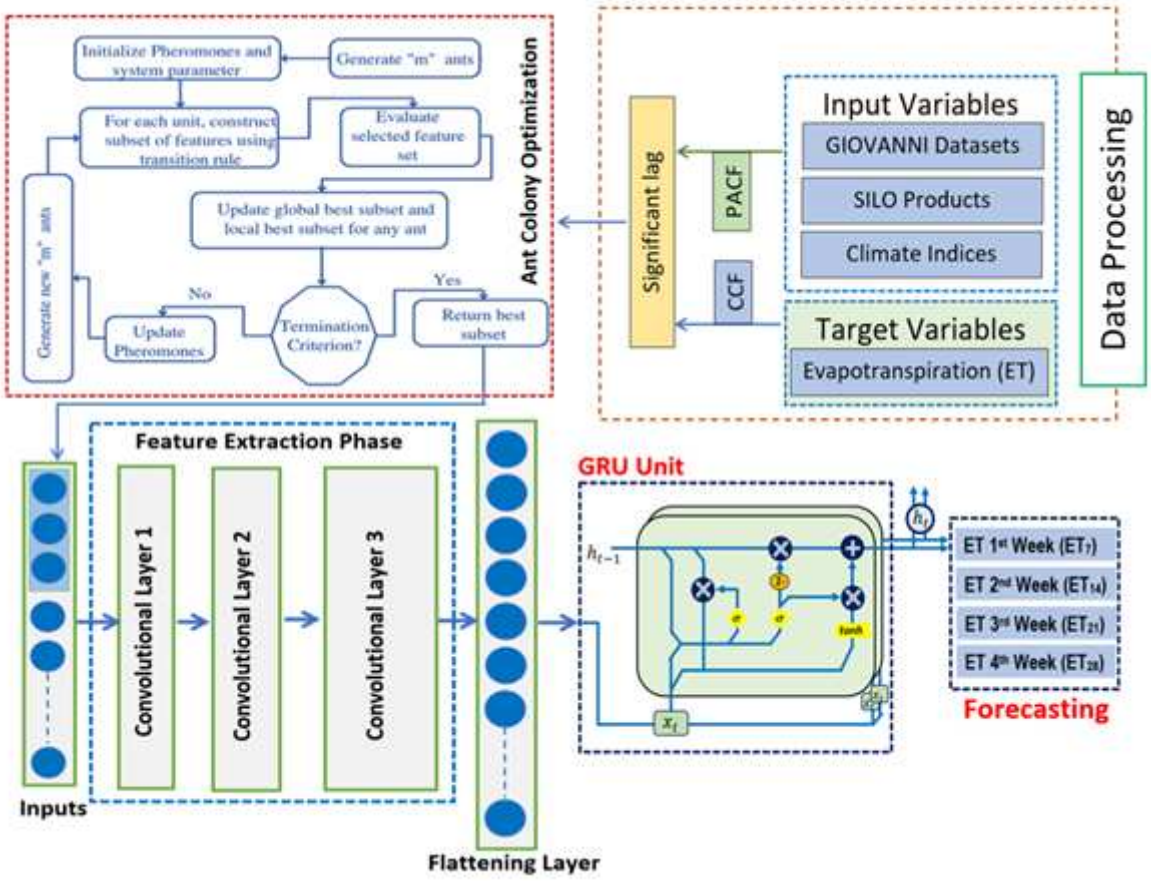


Figure 3

The architecture of CNN model with 2-layered Gated Recurrent Unit for a hybrid CNN-GRU model at week 1–4 ahead ET forecasting with Ant Colony Optimization.

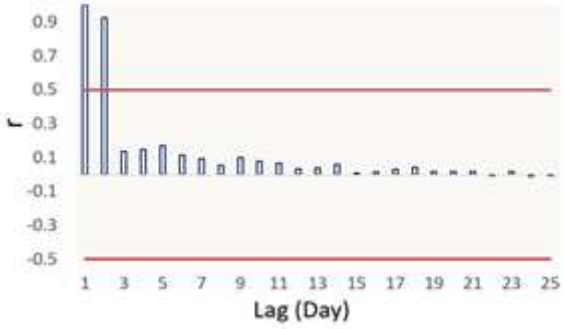


Figure 4

Partial autocorrelation function (PACF) plot of the ET time series exploring the antecedent behaviour in terms of the lag of ET. The red line in the figures indicates the ± 95% confidence level.

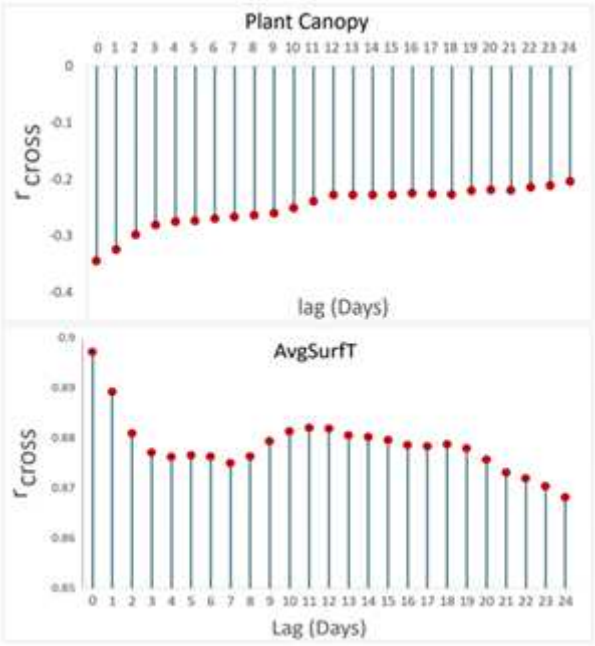


Figure 5

Correlogram shows the covariance between the objective variable (ET) and the predictor variable (plant canopy surface water and average surface skin temperature) in terms of the cross-correlation coefficient for Minendee stations MDB.

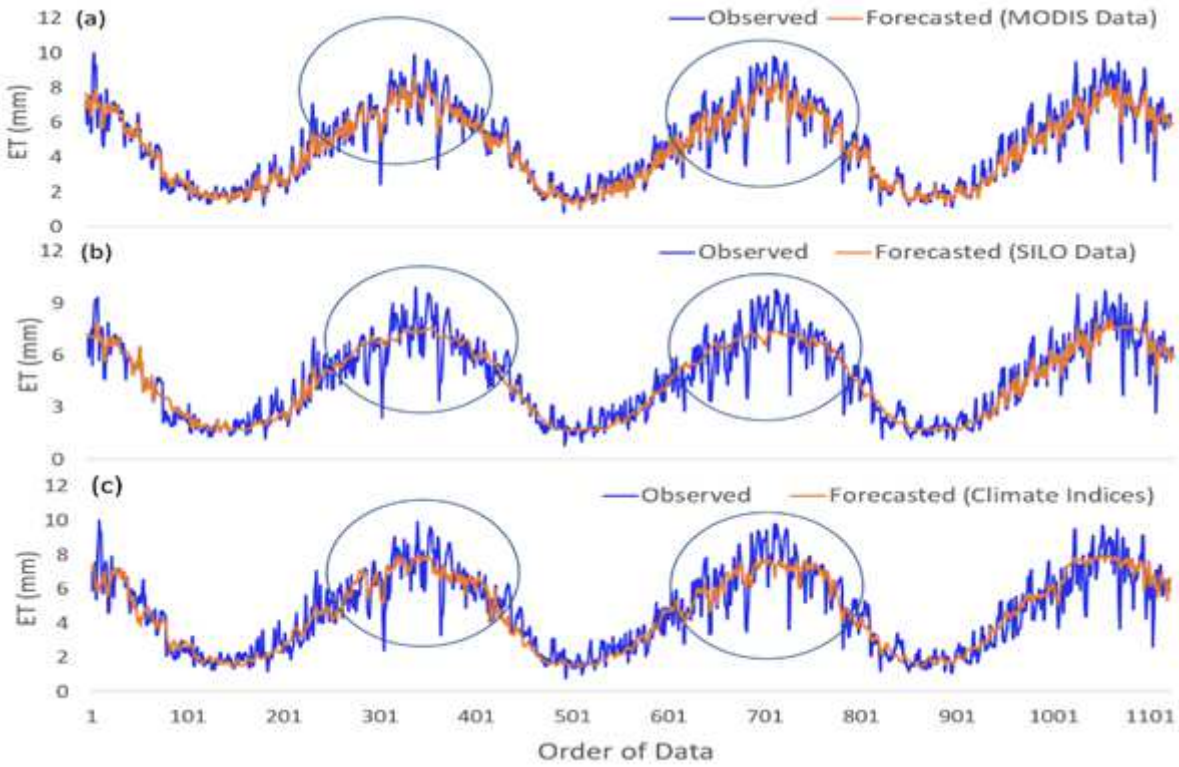


Figure 6

Time series of daily evapotranspiration (ET, mm) for the observed and forecasted ET for the objective model CNN-GRU for (a) MODIS Satellite, (b) SILO data, and (c) Climate mode indices at week 1 lead

forecasting.

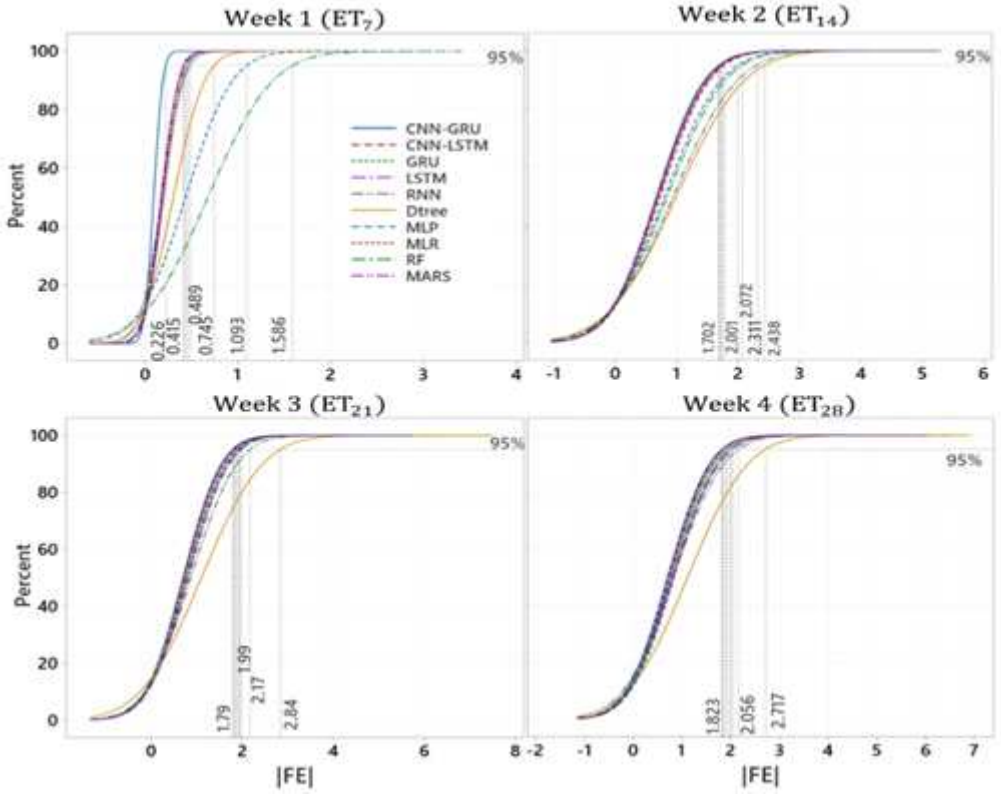


Figure 7

An empirical cumulative distribution function (CDF) plot of |FE| of the CNN-GRU, CNN-LSTM the standalone models (i.e., GRU, LSTM, RNN, MLR, RF etc.) for Menindee station at Week 1, 2, 3, and 4 horizons with Ant Colony Optimization in forecasting ET (mm) of ET forecasting at 95 percentiles on ECDF.

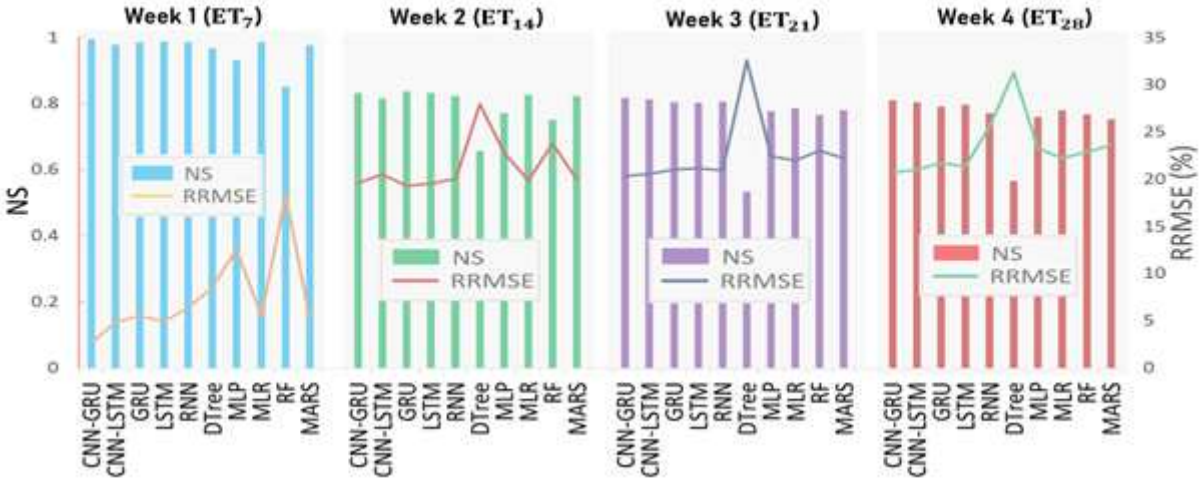


Figure 8

Comparing the forecasting skill of the proposed models in RRMSE (%) and NS in the Menindee station's testing period.

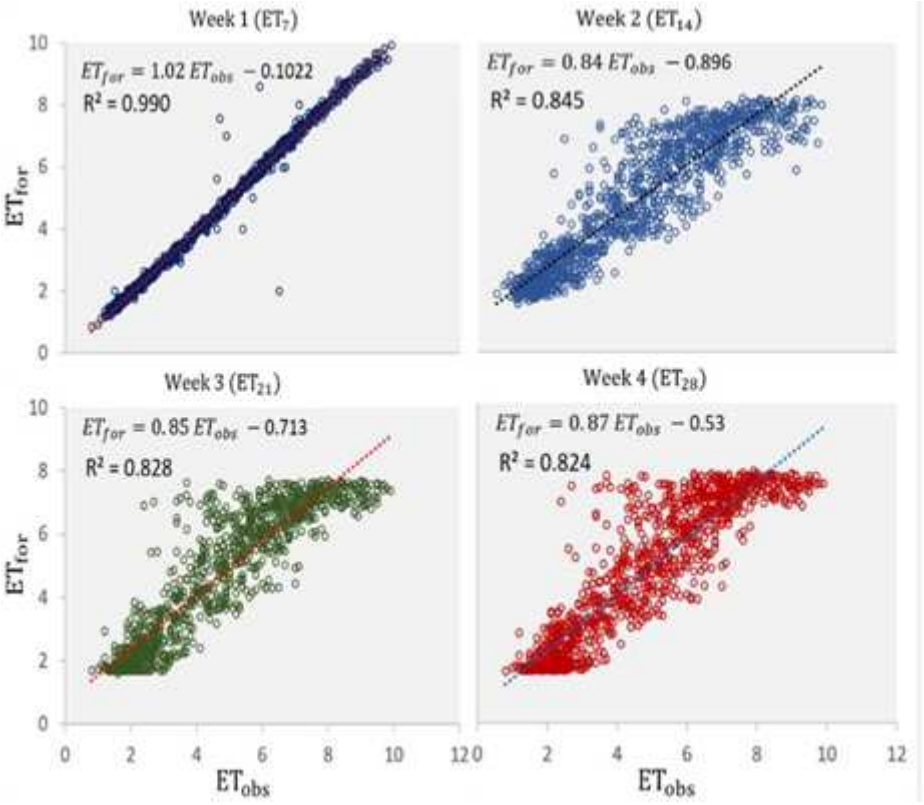


Figure 9

Scatter plot of forecasted with observed ET of Menindee station at Week 1, 2, 3, and 4 horizons) with CNN-GRU model. A least square regression line and coefficient of determination (R2) with a linear fit equation are shown in each sub-panel.

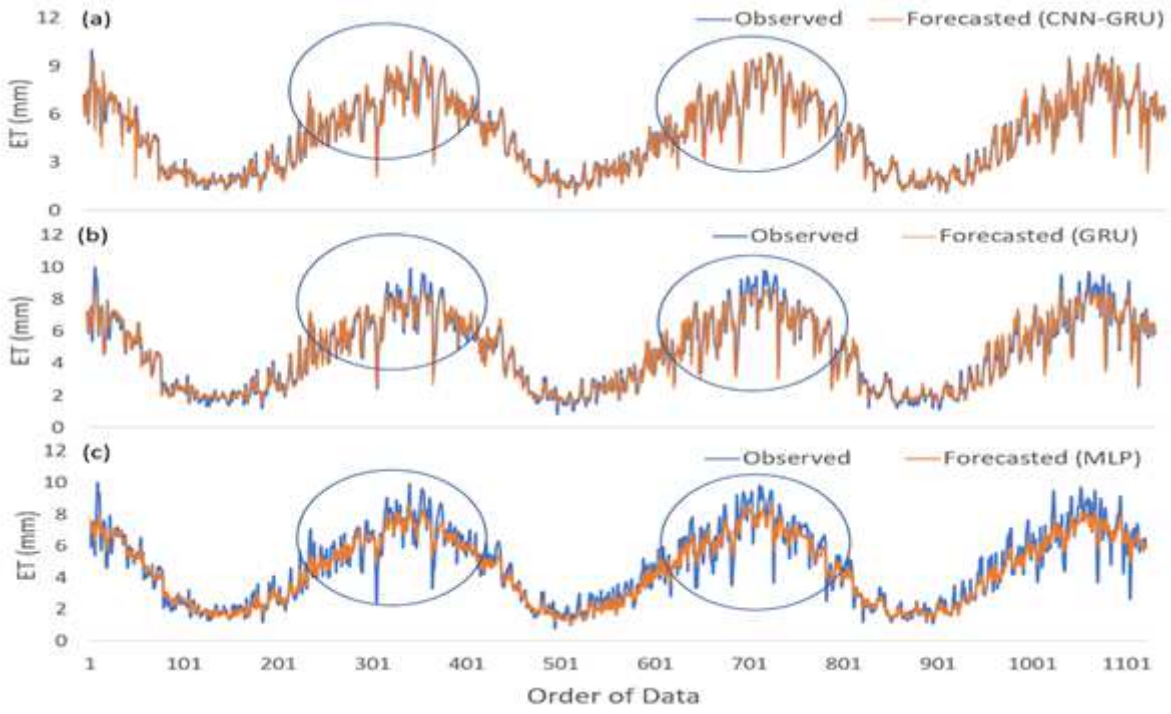


Figure 10

Time series of daily evapotranspiration (ET, mm) for observed and forecasted ET for the (a) objective model (CNN-GRU), (b) standalone GRU and (c) classical MLP at week 1 ahead ET forecast.

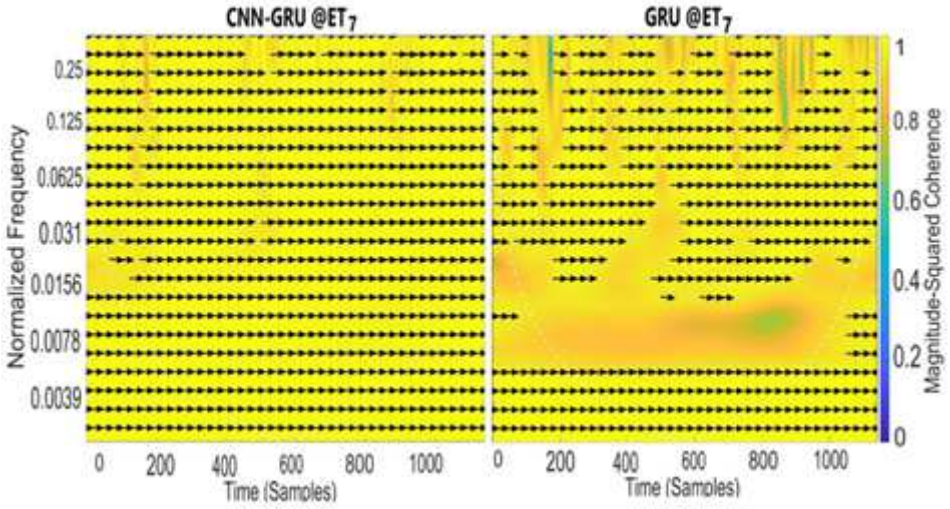


Figure 11

Wavelet coherency spectrums between ETo and ETf using CNN-GRU and GRU model with ACO. The arrows indicate the relative phase relationship within the significant zones of higher correlation.

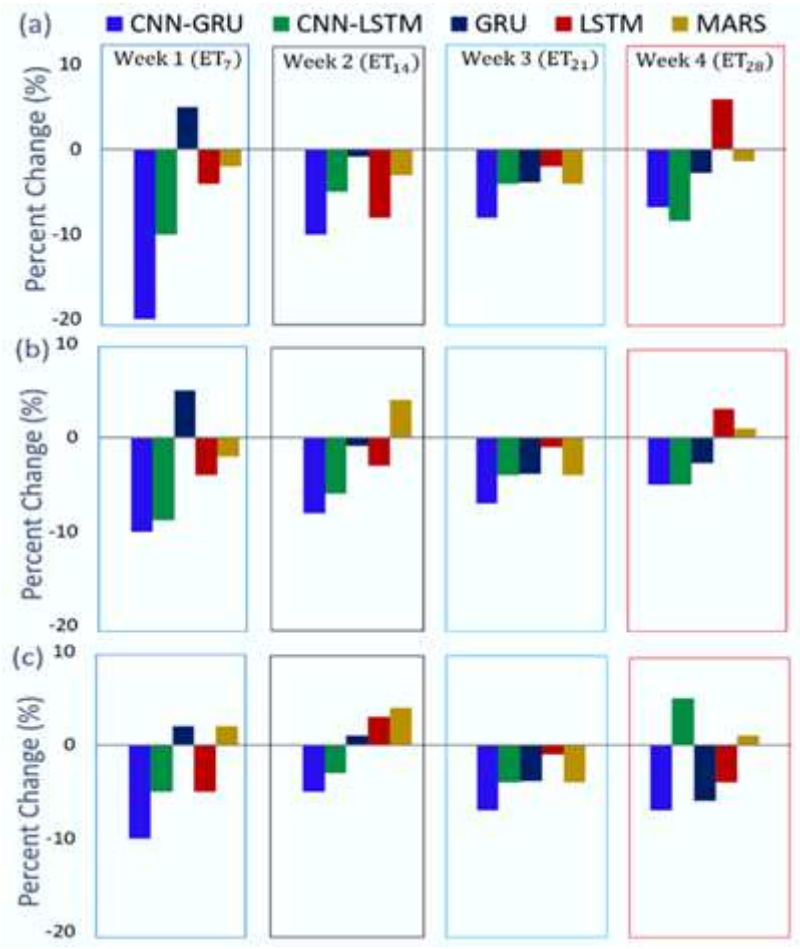


Figure 12

The percentage change in RMAE generated by the objective and benchmark models using the ACO algorithm adopted in forecasting ET at three sites of Murray Darling Basin. (a) Menindee, (b) Fairfield, (c) Gabo Island at different nth (n = 1, 2, 3 and 4) week ahead horizon.